HHS Public Access

Author manuscript

Behav Brain Res. Author manuscript; available in PMC 2023 May 24.

Published in final edited form as:

Behav Brain Res. 2022 May 24; 426: 113844. doi:10.1016/j.bbr.2022.113844.

A dystonia mouse model with motor and sequencing deficits paralleling human disease

Krista Kernodle[a],

Allison M. Bakerian[b],

Allison Cropsey[b],

William T. Dauer[c,d,e],

Daniel K. Leventhal[b,f,g,h,*]

[a]Neuroscience Graduate Program, University of Michigan, Ann Arbor, MI, USA

[b]Department of Neurology, University of Michigan, Ann Arbor, MI, USA

[c]Peter O'Donnell Jr. Brain Institute, University of Texas Southwestern Medical Center, Dallas, TX, USA

[d]Department of Neurology, University of Texas Southwestern Medical Center, Dallas, TX, USA

[e]Department of Neuroscience, University of Texas Southwestern Medical Center, Dallas, TX, USA

[f]Department of Biomedical engineering, University of Michigan, Ann Arbor, MI, USA

[g]Parkinson Disease Foundation Research Center of Excellence, University of Michigan, Ann Arbor, MI, USA

[h]Department of Neurology, VA Ann Arbor Health System, Ann Arbor, MI, USA

Abstract

The dystonias are a group of movement disorders characterized by involuntary twisting movements and postures. A lack of well characterized behavioral models of dystonia has impeded identification of circuit abnormalities giving rise to the disease. Most mouse behavioral assays are implemented independently of cortex, but cortical dysfunction is implicated in human dystonia. It is therefore important to identify dystonia models in which motor cortex-dependent behaviors are altered in ways relevant to human disease. The goal of this study was to characterize a cortically-dependent behavior in the recently-developed Dlx-CKO mouse model of DYT1 dystonia. Mice performed two tasks: skilled reaching and water-elicited grooming. These tests assess motor learning, dexterous skill, and innate motor sequencing. Furthermore, skilled reaching depends strongly on motor cortex, while dorsal striatum is critical for normal grooming. Dlx-

*Corresponding author at: Department of Neurology, University of Michigan, Ann Arbor, MI, USA. dleventh@med.umich.edu (D.K. Leventhal).

CRediT authorship contribution statement

Krista Kernodle: Conceptualization, Software, Validation, Formal analysis, Investigation, Writing – original draft, Visualization. **Allison M. Bakerian:** Investigation. **Allison Cropsey:** Investigation. **William T. Dauer:** Conceptualization, Writing – review & editing, Supervision, Project administration, Funding acquisition. **Daniel K. Leventhal:** Conceptualization, Writing – review & editing, Supervision, Project administration, Funding acquisition.

Appendix A. Supporting information

Supplementary data associated with this article can be found in the online version at doi:10.1016/j.bbr.2022.113844.

CKO mice exhibited significantly lower success rates and pellet contacts compared to control mice during skilled reaching. Despite the skilled reaching impairments, Dlx-CKO mice adapt their reaching strategies. With training, they more consistently contacted the target. Grooming patterns of Dlx-CKO mice are more disorganized than in control mice, as evidenced by a higher proportion of non-chain grooming. However, when Dlx-CKO mice engage in syntactic chains, they execute them similarly to control mice. These abnormalities may provide targets for preclinical intervention trials, as well as facilitate determination of the physiologic path from torsinA dysfunction to motor phenotype.

Keywords

Cortically-dependent behavior; DYT1 dystonia; Endophenotype; Motor learning; TorsinA

1. Introduction

The dystonias are an often-disabling group of movement disorders characterized by involuntary twisting movements and postures. A defining feature of primary dystonia is that there are no other neurological symptoms or CNS damage, making it difficult to model in animals. The discovery of specific gene mutations that cause primary dystonia allowed the creation of animal models with high “construct” validity – that is, they closely recapitulate the human genotype. For example, a 3-base pair in-frame deletion (“ΔE”) mutation in torsinA causes autosomal dominant early-onset generalized primary torsion dystonia [1] (dystonia without other symptoms or neurodegeneration). However, heterozygous torsinA mice (*tor1a*$^{+/-}$) or ΔE knock-in mice (*tor1a*$^{+/\Delta E}$, mimicking the human genotype) do not exhibit a motor phenotype [2]. Mice in which torsinA is globally deleted (*tor1a*$^{-/-}$) or in which the ΔE mutation has been introduced in the endogenous mouse torsinA gene (*tor1a*$^{-/\Delta E}$ & *tor1a*$^{\Delta E/\Delta E}$) all exhibit perinatal lethality and characteristic subcellular nuclear membrane abnormalities [3–5]. These data demonstrate that the ΔE mutation impairs torsinA function, supporting the use of torsinA loss-of-function models for DYT1 dystonia.

DYT1 mouse models with cell-type or region specific torsinA deletion are viable and exhibit specific motor abnormalities. Mice with torsinA conditionally removed from forebrain cholinergic and GABAergic neurons (“Dlx-CKO” mice) are born with no apparent motor abnormalities but as juveniles (post-natal day 14) develop abnormal limb clasping during tail suspension. The onset of these movements corresponds with the selective loss of striatal cholinergic interneurons (ChIs) in the dorsal striatum [6]. The relationship between hindlimb clasping and dystonia in humans remains unclear, however.

Cortical dysfunction is strongly implicated in dystonia pathophysiology. Human dystonia is often induced or exacerbated by voluntary movement, perhaps due to “overflow” in sensorimotor cortical regions from desired activation patterns. Cortical inhibition is reduced in humans with dystonia, suggesting that this abnormality may contribute to recruitment of topographically adjacent motor cortical regions during movement [7,8]. These data indicate a central role for cortical dysfunction in dystonia, but most behavioral assays in mice are implemented independently of cortex [9,10]. For example, simple lever press tasks and

rodent grooming are not affected by cortical lesions [9,11]. On the other hand, dexterous skills requiring finely controlled multi-joint and digit coordination are highly sensitive to cortical lesions [10,12], and impaired in human dystonia [13–15].

Given the cortical abnormalities observed in humans with dystonia, we explored the ability of Dlx-CKO mice to perform skilled reaching, which depends critically on motor cortex [12]. Conversely, water-elicited grooming reliably induces highly stereotyped behavior in mice that depends on striatum, but not cortex [11,16,17]. By using both tasks, we therefore assessed motor learning, dexterous skill, and innate motor sequencing, allowing us to characterize behaviors in Dlx-CKO mice that rely on distinct forebrain structures implicated in human dystonia. Given the evidence of cortical dysfunction and impaired dexterity in human dystonia, we hypothesized that Dlx-CKO mice are impaired in both learning and performing skilled reaching. Conversely, we predicted that grooming patterns would be normal in Dlx-CKO mice based on their preserved performance of other non-cortically dependent tasks [6].

2. Materials and Methods

2.1. Experimental overview

To evaluate the performance of Dlx-CKO mice on cortex and striatum-dependent tasks, mice underwent three sessions of induced grooming, 21 sessions of skilled reaching, and a final session of induced grooming (Fig. 1A). All mice were housed on a reverse light-dark cycle (7 AM – 7 PM), and all behavioral experiments were performed in the early afternoon during the dark phase.

2.2. Mice

All animal procedures were approved by the University of Michigan Institutional Animal Care and use Committee. Numbers of mice included in each experimental group and analysis are indicated in figure legends. Dlx-CKO mice were generated by crossing Cre^{+} $tor1a^{+/-}$[6] with $tor1a^{flx/flx}$ mice [18], using the breeding strategy described in [6]. Mice with genotype $tor1a^{flx/+}$ were used as age and sex matched littermate controls. At the time of the first skilled reaching session, Dlx-CKO mice had a mean age of 193 days (range 112–388 days) and control mice had a mean age of 195 days (range 117–388 days). At that time, the mean weight of Dlx-CKO mice was 28.4 g (range 23–36 g), and the mean weight of control mice was 28.1 g (range 21–39 g). Male (control=5, Dlx-CKO=5) and female (control=9, Dlx-CKO=4) mice were housed in groups of 2–3. Food restriction was imposed on all animals during the training and testing periods of the skilled reaching task for no more than 6 days in a row such that animals' weights were maintained ≥ 90% of their free-feeding weight. Water was available ad libitum in their home cages. 5 Dlx-CKO mice experienced seizures and were excluded from the study. 4 had started grooming but not skilled reaching; 1 had started skilled reaching. In each case, they were removed from the experiment as soon as seizures were noted and excluded from all analyses. In addition, 2 control mice that no longer had littermate-matched Dlx-CKO mice were excluded from all analyses.

2.3. Grooming

Mice were placed in an acrylic cylinder (15 cm diameter × 20 cm height). A camera was mounted to the platform and focused on the cylinder. Two mirrors were positioned on the left and right to allow clear views of the mouse from multiple angles. Videos of the entire session were recorded. Before each trial, mice were lightly sprayed with water on the face and whiskers, then placed into the cylinder. Mice were allowed to move freely, and grooming behaviors were spontaneous. Trials lasted for a total of 15 min, with two trials constituting a session. Each mouse performed one grooming session per week for three weeks prior to beginning the skilled reaching task. Mice performed one additional session of grooming after the final training session in the skilled reaching task.

2.4. Skilled reaching

2.4.1. Automated reaching system—Training and testing were carried out in custom-built skilled reaching chambers built similarly to those described in [19], with two main differences. First, the reaching slot did not extend to the bottom of the front panel. Instead, the bottom of the reaching slot (10 mm × 7 cm) was 17.5 mm from the floor. This was to prevent the mouse from grasping for the pellet before the pedestal was fully elevated. Second, the pellet was delivered on a “pellet delivery rod” – a pedestal that moved vertically through a reservoir of sugar pellets (20 mg Dustless Precision Pellets, Bio-Serv, Flemington, New Jersey). This allowed the task to be automated [20], but contrasts with the shelf on which reward pellets were manually placed in [19]. A linear actuator with potentiometer feedback (Actuonix, Saanichton, Canada) was connected to the acrylic pellet delivery rod and mounted in a custom frame below the support box. Before each session, the pellet delivery rod was positioned 1 cm from the front of the reaching slot, and aligned with the right or left edge of the slot according to each mouse’s paw preference. Individual pellets were therefore located approximately 1 cm from the front of the chamber. Videos of the entire session were recorded by a camera mounted in front of the reaching slot. A mirror was placed on either side of the front of the reaching chamber and angled to allow side views of the paw during reaching.

2.4.2. Trial performance—A custom-built Arduino (Arduino Mega 2560 Rev3, Arduino, Boston, MA) based system controlled the experiment. Each training session began with the pellet delivery rod at the lowest position inside the funnel. When a session began, the pellet delivery rod rose to the bottom of the reaching slot, triggering an LED to indicate the start of a trial. The delivery rod remained in place for 3 s before lowering, triggering the LED to turn off. This began an intertrial interval of ~5 s wherein the pellet delivery rod retracted into the funnel to pick up a new pellet, then rose for a new trial.

2.4.3. Habituation—The purpose of habituation is to familiarize mice with the reaching chamber and sucrose reward pellets. Habituation lasted for three sessions, each 20 min in length. Mice were placed on food restriction and introduced to the sucrose reward pellets in their home cages 24 h prior to the first day of habituation. On day 1 of habituation, a pile of 10 pellets was placed in the skilled reaching chamber to encourage exploration. On days 2 and 3 of habituation, mice received no sucrose pellets, and the skilled reaching apparatus was turned on for 5 min in each session to familiarize mice with the sound.

2.4.4. Pre-training—During 'pre-training', mice were evaluated for reaching paw-preference and trained to reach for the linear actuator. Paw preference and training mice to reach for the linear actuator was performed as in [20]. To entice the mice to reach for the actuator, the investigator held a pellet in forceps and gradually withdrew it from the chamber until the mice reached for it with their forepaw. Once mice reached for the delivery rod 10 times without being baited by the experimenter, they began training on the automated task. Training initially occurred in a "manual" mode in which the investigator could raise/lower the pedestal by pushing a button. This allowed us to control the duration that the actuator was in "reaching position" (aligned with the bottom of the slot) until the mice began to consistently reach. We gradually decreased trial length to 3 s, at which point the actuator was set to "automatic" mode. In this mode, the pedestal remained in reaching position for 3 s before being lowered for 5 s. Pre-training was complete once mice performed 20 trials with reaches in a single session (30 min) with the actuator on "automatic".

2.4.5. Training—After pre-training, mice began 30-min training sessions with the automated system, in which they could perform as many reaches as possible. Sessions were not cut short at a prespecified number of trials. Mice were trained for 5 days per week for a total of 21 sessions. Videos were captured of the entire training session. All videos were recorded at 100 frames-per-second and 1920 × 1080 pixels by a high-definition color digital camera (HBLK-6FT-0309, Panasonic, Kadoma, Japan).

2.5. Grooming sequence analysis

Behavioral analysis consisted of frame-by-frame video scoring to assess bout and syntactic chain onset. A single bout is continuous grooming without long pauses. A pause occurs when the mouse stops grooming briefly (<6 s) but quickly resumes without performing locomotor activity [17]. Behaviors performed throughout bouts were assigned numerical values: 0 – no grooming present; 1 – small, elliptical strokes about the mouth and nose (Phase 1); 2 – asynchronous, unilateral strokes increasing in amplitude from vibrissae to the eyes and occasionally the ears (Phase 2); 3 – synchronous, bilateral strokes involving both forepaws from the vibrissae to the eyes and ears (Phase 3); 4 – licking of the torso or haunches (Phase 4); 5 – licking of the forepaws that does not include elliptical strokes. Syntactic chain onset was defined as initiation of Phase 1 grooming that progressed to Phase 2 or Phase 3. All other grooming was defined as non-chain. A complete chain progressed through Phase 1, Phase 2 and/or Phase 3, and Phase 4 [21]. Phase transitions performed within syntactic chains were grouped into typical and atypical transitions. Typical transitions consist of those from phases 1→2, 2→3, 3→4, and 4→0 (here 0 represents no grooming). All other transitions were considered atypical and can be broken into three groups: skips (e.g., 2→4), reverses (e.g., 4→3), and premature termination (e.g., 3→0) [17]. Frame number was recorded for bout initiation, bout end, syntactic chain initiation, and syntactic chain end.

Time spent grooming for each session was calculated by dividing total time grooming (sum of all individual bout and syntactic chain durations) by the total trial time. Time spent performing non-chain grooming was calculated by subtracting the time spent performing syntactic chains from their respective bouts (isolating non-chain grooming time), then

dividing by the total trial time. Time spent performing chain grooming for each session was calculated by dividing the sum of all individual chain durations by the total trial time (Fig. 5A). Initiations per minute of grooming were calculated for each session by taking the number of non-chain bouts initiated, syntactic chains initiated, or both (total) and dividing it by the time spent grooming in minutes (Fig. 5B). Chain duration was measured from onset of Phase 1 through the end of Phase 4 [11]. Non-chain grooming bout duration was calculated by subtracting the duration of any syntactic chains within a grooming bout from the total bout duration. Distributions of bout durations were compared to determine if the durations of individual bouts differed between experimental groups. Non-chain bout durations were grouped into bins of 5 s; syntactic chain durations were grouped into bins of 3 s (Fig. 5C, D). Chain completion rates were calculated per session by dividing the number of complete chains by the number of chains initiated (Fig. 5E). The number of occurrences of each grooming phase per trial was calculated for each mouse, then averaged across mice (Fig. 5F).

2.6. Skilled reaching analysis

Skilled reaching videos were segmented into individual videos for each trial and assigned random codes so that scorers were blinded to the mouse's genotype and day of testing. Reach outcome for each trial was scored by visual inspection as follows: 0 – no pellet presented or other mechanical failure; 1- first attempt success (obtained pellet on initial limb advance); 2 – obtained pellet by reaching, but not on first attempt; 3 – forelimb advanced, pellet was grasped then dropped in the box; 4 – forelimb advanced, but the pellet was knocked off the pedestal ('pellet displaced'); 5 – the mouse reached but the pellet remained on the pedestal ('pellet remained'); 6 – pellet was obtained using its tongue; 7 – the mouse did not perform any reaches; 8 – the mouse used its non- preferred paw to reach; 9 – obtained pellet with use of both paw and tongue. Outcome percentages were calculated by dividing the number of trials of each outcome by the total number of trials per session. For comparison of failure mechanisms in skilled reaching, 'unsuccessful' trials were defined as trials where a reach was performed but no reward pellet obtained (scores 3, 4, and 5).

Success rate was calculated for each session by dividing the total number of successful trials (scores 1 and 2) by the total number of trials with reaches (sum of scores 1, 2, 3, 4, and 5) (Fig. 2A, B). The rates of 'pellet displaced' and 'pellet remains' trials were calculated by dividing the number of pellet displaced and pellet remains trials (scores 4 and 5, respectively), by the total number of unsuccessful trials (sum of scores 3, 4, and 5) (Fig. 2D). Only sessions in which mice actively reached during at least 20 trials were included in analyses of success rate and failure mechanism (Fig. 2B, D). This eliminated 13 control and 29 Dlx-CKO sessions. All sessions were included in the analysis of number of trials with reaches (Fig. 2A).

Semi-quantitative sub-movement analysis was performed for each mouse in the skilled reaching experiment on the first three successful reaches during the first 5 days of training (early training) and the last three successful reaches during the final 5 days of training (late training). Behavioral analysis consisted of frame-by-frame video scoring to assess the presence of 12 reaching movement elements that have been described in detail [22]. Briefly,

these include “orient” (head and snout directed towards the pellet), “limb lift”, “digits close” (digits partially flex as the paw supinates into vertical orientation), “aim”, “digits extend and open”, “pronate” (occurs as digits extend over the food), “grasp”, “supinate I” (paw supinates to vertical to retreat through the slot), “supinate II” (palm faces the mouth), “release” (into the mouth), and “replace” (paw is placed back on the floor). Each movement is scored as 0 (normal), 0.5 (present but abnormal), or 1 (absent).

2.7. Statistics

To test whether skilled reaching had an effect on grooming, a Welch’s two sample t-test (using R *t.test*) was used to compare grooming outcomes before and after skilled reaching. Given the similarity in grooming outcomes pre- and post-reaching (total time spent grooming: $t(14) = 0.086$, $p = 0.93$; time spent non-chain grooming: $t(14) = 0.088$, $p = 0.93$; time spent chain grooming: $t(11) = 0.042$, $p = 0.97$), further analyses combined all 4 sessions of grooming. A linear regression model (using R *glm*) was used to evaluate time spent grooming with genotype as the independent variable. The Kruskall-Wallis test by ranks (using R *kruskal.test*) was used to examine differences of genotype on grooming initiation rates (Fig. 5B) as well as grooming stroke type (Fig. 5F). A Poisson regression model was implemented (using R *lmer*) for chain completion (offset by number of chains; Fig. 5E), transition type (offset by number of chains; Supplemental Fig. 2A), and atypical transition type (offset by the number of atypical transitions; Supplemental Fig. 2B) due to the count nature of the data.

Linear mixed-effects models were used to evaluate success and failure rates in skilled reaching. We implemented linear mixed-effects models (using R *lmer*) with random intercepts/effects for each mouse (where effect of session varied between mice) and main interaction effects of genotype and session number. Linear mixed-effects models included averages for all 21 sessions of training for all mice. A linear mixed-effects model with the fixed effect of session number and a random effect for the interaction between genotype and session number was used to identify differences between groups on specific training days.

Two-way mixed-effects ANOVAs were performed to evaluate the effect of genotype and training on each of the 12 reaching movement elements. We implemented two-way mixed-effects ANOVA models (using R *anova_test*) with training as the within subjects-variable and genotype as the between-subjects variable. Two-way mixed-effects ANOVA models included averages for each training group (“early” vs “late”) for all mice. Pairwise t-tests with Bonferroni correction (using R *pairwise_t_test*) were used to evaluate the effect of either training or genotype on each movement element.

3. Results

We tested control and Dlx-CKO mice on two tasks designed to assess motor learning (skilled reaching), dexterous skill (skilled reaching), and innate motor sequencing (grooming). Each mouse underwent the same sequence of behavioral assays (Fig. 1A): three sessions of induced grooming, 21 sessions of skilled reaching, and a final session of induced grooming.

3.1. Skilled reaching deficits suggest a primary motor impairment in Dlx-CKO mice

The single-pellet skilled reaching task was used to examine motor learning as well as dexterous skill performance. Skilled reaching is a cortically-dependent task in which mice are trained to reach for and grasp small sugar pellets from a pedestal (Fig. 1B). Dlx-CKO mice performed slightly fewer reaching trials than control mice, though both groups performed large numbers of reaches (Fig. 2A). Almost all attempts at pellet retrieval were made with the preferred forelimb (as opposed to the tongue or non-preferred forelimb, Supplemental Fig. 1). Successful pellet retrieval requires accurate paw transport to the pellet followed by precise, coordinated hand and digit movements that are acquired with practice [12,23]. Dlx-CKO mice were consistently less successful obtaining sugar pellets than controls, suggesting a deficit in motor execution, motor learning, or both (Fig. 2B).

Learning is typically assessed by changes in the number of successfully retrieved pellets divided by the total number of attempts (success rate). However, success rates did not change with training in our task (Fig. 2B). To assess learning in greater detail, we examined the frequency of two distinct failure mechanisms. The first is trials in which the mouse knocked the pellet off the pedestal (Fig. 2C, Top: “pellet displaced”). This is in contrast to trials in which the mouse makes little or no contact with the pellet, failing to knock it from the pedestal (Fig. 2C, Bottom: “pellet remains”). As training progressed, Dlx-CKO mice exhibited a higher proportion of “pellet displaced” trials and a lower proportion of “pellet remains” trials (Fig. 2D). This suggests that Dlx- CKO mice are capable of motor learning. The inability to accurately target the pellet suggests that Dlx-CKO mice have a primary impairment in postural control and/or proximal limb movement that interferes with the “transport” phase of skilled reaching [24].

To identify qualitative differences between reach-to-grasp movements in Dlx-CKO and control mice, we scored reaches on a semi-quantitative movement rating scale before and after training [22,25]. This scale evaluates the presence or absence of submovements in the reach-to-grasp sequence. For the most part, both groups performed all submovements, even early in training (Fig. 3). The exception is paw pronation as it extends towards the pellet, which was inconsistently present in both groups. There were few significant differences between Dlx-CKO and control mice in submovement performance. Control mice more consistently performed “supinate I” after training, where the paw supinates after grabbing the pellet prior to retraction through the slot. There were other statistically significant differences between genotypes (e.g., “digits extend and open” changed for control but not Dlx-CKO mice after training), but the absolute differences in scores were small. Thus, there are no obvious gross differences between reach-to-grasp submovements in Dlx-CKO and control mice that would account for the difference in success rates.

3.2. Grooming sequences are disrupted in Dlx-CKO mice

Skilled reaching is sensitive to cortical lesions but may also be impaired with subcortical lesions. We therefore also characterized grooming behavior, which is insensitive to cortical lesions but sensitive to striatal lesions [11]. Grooming is an innate behavior with a patterned, sequential organization that starts at the nose and progresses across the body in a cephalocaudal pattern [21]. About 10–15% of grooming is composed of highly stereotyped

and ordered movements called a syntactic chain [17]. Syntactic chains have distinct phases that follow an expected progression from 1 to 4 and are usually embedded in more flexible non-chain grooming bouts (Fig. 4). Adherence to chain syntax is low in models with altered cerebellar and striatal physiology, with shorter more frequent non-chain bouts being common [26,27].

We performed grooming assessments before and after skilled reaching training to test whether skill learning would affect grooming performance. However, there was no effect of session (pre-skilled reaching versus post-skilled reaching) on grooming outcomes between groups (see 2.7. Statistics). Therefore, all analyses are collapsed across sessions. Dlx-CKO and control mice performed similar amounts of grooming, but grooming structure was less organized in Dlx-CKO mice. There was not a significant difference in the time spent grooming (in total or separated into chain and non-chain grooming) or total number of bouts initiated between groups (Fig. 5A,B). However, Dlx-CKO mice initiated fewer syntactic chains, defined as phase 1 grooming that progresses to phase 2 or 3 [28] (Fig. 5B). Dlx-CKO mice performed similar total (chain plus non-chain) amounts of unilateral and bilateral strokes compared to control mice, but fewer ellipses (Fig. 5F). Consistent with previous results, neither control nor Dlx-CKO mice performed multiple, fast elliptical strokes outside of syntactic grooming [28]. Thus, Dlx-CKO mice progressed normally through syntactic chains once they were initiated. (Fig. 5E, Supplemental Fig. 2). Finally, there was no effect of genotype on the duration of non-chain or chain grooming bouts (linear regression, effect of genotype on duration of: non-chain bouts: $t(12) = 0.029$, $p = 0.98$; syntactic chains: $t(12) = \_ 1.44$, $p = 0.18$). The distributions of the durations of non-chain and chain grooming bouts were similar between groups, providing further evidence that individual grooming bouts of the same type (chain vs non-chain) were similar between Dlx-CKO and control mice (Fig. 5C, D). Taken together, these findings indicate that the temporal structure of grooming is more variable in Dlx-CKO mice, as more of their grooming was spent in unstructured non-chain bouts.

4. Discussion

Our results suggest that Dlx-CKO mice have primary impairments in coordination and manual dexterity. Dlx-CKO mice had significantly lower success rates and pellet contacts compared to control mice on the skilled reaching task, though both groups improved their reaching accuracy. Our grooming experiment identified deficits in sequence initiation, but not sequence progression. These results are reminiscent of endophenotypes seen in human dystonia and may provide a mechanism to dissect the physiologic path from torsinA dysfunction to motor phenotype.

There are several potential explanations for skilled reaching impairments in Dlx-CKO mice. First, Dlx-CKO mice performed fewer reaches than control mice, and therefore had less practice. A motivational/practice deficit is unlikely to explain their performance for several reasons, however. First, Dlx-CKO mice performed comparable (or larger) numbers of reaches compared to other mouse skilled reaching experiments [19,29], and only about 8% fewer reaches than control mice in these experiments. Second, both groups of mice became more accurate with their reaches on a similar time scale (Fig. 2D). Our results instead

suggest that Dlx-CKO mice have at least a primary motor deficit, and possibly a sensory deficit. Rodents use their whiskers to identify the reaching slot [30], and a combination of olfaction and prior experience to localize the pellet [31,32]. However, the reach itself is ballistic with little or no online adjustment. Motor cortex is essential for ballistic movements during the transport phase of reaching, while sensory information influences grasping and food release [24,33]. Dlx-CKO mice frequently missed the pellet entirely (Fig. 2D), and therefore had limited opportunities to use somatosensory feedback to adjust reaches. Our results are therefore more consistent with primary motor rather than sensory deficits, though we cannot completely exclude the latter. Future experiments designed to explore sensory deficits independent of skilled reaching in Dlx-CKO mice may provide additional clarity.

Neither control nor Dlx-CKO mice exhibited statistically significant increases in their success rates in our task, preventing us from identifying motor learning deficits based on success rates. However, Dlx-CKO and control mice increased the number of “pellet displaced” trials with training, suggesting that they were adapting their reaching strategies (Fig. 2D). The stable, and relatively low, success rates were likely related to task design. In many versions of skilled reaching, mice retrieve pellets from a shelf, allowing them to slide the pellet into the chamber. Because our task used a pedestal, the mice had to both locate and securely grasp the pellet to prevent it from falling between the pedestal and the front of the chamber. In another pedestal-based skilled reaching task, success rates were 32 + /− 9.9% for freely behaving mice [29], similar to the ~20% success rate for control mice in this study. The slightly higher success rate in that study may be related to details of the chamber design; their reaching slot extends all the way to the floor so that mice do not have to lift their paw before advancing it. Rats had higher success rates on similar pedestal-based tasks [23,34], but this may be because of their larger paws or inter-species differences in fine motor control. Whether the mice in the current study would have improved their grasping to increase success rate with further training is uncertain. Regardless, the change in the rate of pellet displacement strongly suggests the engagement of motor learning. This is consistent with previous results on the accelerating rotarod, in which Dlx-CKO mice showed normal improvement [6]. On the rotarod, however, there was no difference between Dlx-CKO mice and controls in baseline performance, suggesting that skilled reaching is a more sensitive assay of motor impairment for Dlx-CKO mice.

We found at most subtle differences between Dlx-CKO and control mice on the semiquantitative submovement rating scale. These results indicate that the reduced success rates for Dlx-CKO mice are unlikely to be due to an elemental motor deficit. That is, Dlx-CKO mice were capable of performing forelimb extension, forelimb pronation/supination, digit flexion/extension, and other submovements. This argues that their motor impairment may be related to coordinating/timing these submovements with respect to each other. The most impaired submovement in both groups was paw pronation. This could be related to task design or the species under study, as the rating scale was developed for rats performing a shelf-based task. In a nearly identical pedestal-based rat task [35], pronation was well-preserved, suggesting that the relative absence of pronation is specific to mice.

Chain grooming is strongly dependent on basal ganglia function. Striatal lesions disrupt syntactic chain completion and syntax without affecting syntactic chain initiation rates [11].

Similar patterns are caused by cortical and cerebellar lesions, albeit transiently [11]. This is different from our results, wherein Dlx-CKO mice maintained syntactic chain completion rates and syntax but decreased syntactic chain initiations (Fig. 5B, E). These results suggest the striatal control of chain syntax remains largely intact for Dlx-CKO mice, at least once a chain is initiated. Why syntactic chain initiation was reduced remains unclear. One possibility is that network dysfunction in Dlx-CKO mice affects motor sequencing in ways distinct from focal lesions in cortex, striatum, or cerebellum. Functional connectivity among the striatum, cortex, thalamus, and cerebellum are increased in Dlx-CKO mice, suggesting widespread changes in motor circuits that extend beyond local dysfunction [36]. Another non-exclusive possibility is that altered basal ganglia output specifically impairs chain grooming initiation. While dorsal striatal activity signals transitions between chain grooming phases (but not non-chain grooming phases), SNr activity tends to signal the start of a chain [37,38]. Basal ganglia output is abnormal in dystonia, with low frequency bursty, oscillatory firing patterns [39–41], raising the possibility that disrupted SNr output interferes with chain initiation in Dlx-CKO mice. Direct SNr recordings will be needed to test this hypothesis. If nigral firing patterns are indeed abnormal in Dlx-CKO mice, the next step would be to identify the upstream cause of these changes. Striatal cholinergic dysfunction has been observed in Dlx-CKO mice [6], though the precise mechanisms through which this could lead to abnormal basal ganglia output are unknown.

Progress on understanding the pathophysiology of dystonia has been limited by the availability of mouse models with clear phenotypes (see [42] for review). Mouse models mimicking the human DYT1 genotype (heterozygous *tor1a*$^{\Delta E/+}$) or over expressing human mutant torsinA display motor deficits in the beam walking task but inconsistent performance on the rotarod task [3,43–45]. Inconsistent results have also been found in mouse models with brain region specific torsinA deletion, with some displaying deficits in beam walking but normal rotarod performance [6,46–48], and yet others with normal beam walking but impaired rotarod performance [49]. These inconsistencies complicate understanding the relevance to human dystonia. Here, we have shown that Dlx-CKO mice have specific motor deficits with parallels in human dystonia [13–15]. It is not known if impaired dexterity in humans with dystonia responds to treatment (e.g., DBS or anticholinergics), or if other DYT1 models also have impaired manual dexterity. Nonetheless, these clear abnormalities in skilled reaching could be targets for preclinical therapeutic trials and be used to establish physiology-phenotype correlations. Similarly, DYT1 carriers have abnormalities in motor sequencing, though this is true of both manifesting and non-manifesting carriers [50]. The abnormal sequence initiation in grooming patterns that we observed therefore parallels motor sequence deficits in human dystonia and may provide a mechanism to dissect the physiology underlying this endophenotype.

In conclusion, Dlx-CKO mice display primary motor deficits and motor sequencing abnormalities with parallels in human DYT1 dystonia. These abnormalities may provide targets for preclinical intervention trials, as well as facilitate determination of the physiologic path from torsinA dysfunction to motor phenotype.

Supplementary Material

Refer to Web version on PubMed Central for supplementary material.

Acknowledgements

Funding for this work was provided by the National Institute of Health [grant number R01NS109227].

Abbreviations:

ChIs	cholinergic interneurons
CNS	central nervous system
SNr	substantia nigra pars reticulata
tor1a	murine torsinA gene

References

[1]. Ozelius LJ, Hewett JW, Page CE, Bressman SB, Kramer PL, Shalish C, de Leon D, Brin MF, Raymond D, Corey DP, Fahn S, Risch NJ, Buckler AJ, Gusella JF, Breakefield XO, The early-onset torsion dystonia gene (DYT1) encodes an ATP-binding protein, Nat. Genet 17 (1997) 40–48, 10.1038/ng0997-40. [PubMed: 9288096]

[2]. Tanabe LM, Martin C, Dauer WT, Genetic background modulates the phenotype of a mouse model of DYT1 dystonia, PloS One 7 (2012), e32245, 10.1371/journal.pone.0032245.

[3]. Dang MT, Yokoi F, McNaught KSP, Jengelley T-A, Jackson T, Li J, Li Y, Generation and characterization of Dyt1 DeltaGAG knock-in mouse as a model for early-onset dystonia, Exp. Neurol 196 (2005) 452–463, 10.1016/j.expneurol.2005.08.025. [PubMed: 16242683]

[4]. Goodchild RE, Kim CE, Dauer WT, Loss of the dystonia-associated protein torsinA selectively disrupts the neuronal nuclear envelope, Neuron 48 (2005) 923–932, 10.1016/j.neuron.2005.11.010. [PubMed: 16364897]

[5]. Dang MT, Yokoi F, Cheetham CC, Lu J, Vo V, Lovinger DM, Li Y, An anticholinergic reverses motor control and corticostriatal LTD deficits in Dyt1 ΔGAG knock-in mice, Behav. Brain Res 226 (2012) 465–472, 10.1016/j.bbr.2011.10.002. [PubMed: 21995941]

[6]. Pappas SS, Darr K, Holley SM, Cepeda C, Mabrouk OS, Wong J-MT, LeWitt TM, Paudel R, Houlden H, Kennedy RT, Levine MS, Dauer WT, Forebrain deletion of the dystonia protein torsinA causes dystonic-like movements and loss of striatal cholinergic neurons, ELife 4 (2015), e08352, 10.7554/eLife.08352.

[7]. Quartarone A, Hallett M, Emerging concepts in the physiological basis of dystonia: emerging concepts in the basis of dystonia, Mov. Disord 28 (2013) 958–967, 10.1002/mds.25532. [PubMed: 23893452]

[8]. Sohn YH, Hallett M, Surround inhibition in human motor system, Exp. Brain Res 158 (2004) 397–404, 10.1007/s00221-004-1909-y. [PubMed: 15146307]

[9]. Kawai R, Markman T, Poddar R, Ko R, Fantana AL, Dhawale AK, Kampff AR, Ölveczky BP, Motor cortex is required for learning but not for executing a motor skill, Neuron 86 (2015) 800–812, 10.1016/j.neuron.2015.03.024. [PubMed: 25892304]

[10]. Basista MJ, Yoshida Y, Corticospinal pathways and interactions underpinning dexterous forelimb movement of the rodent, Neuroscience 450 (2020) 184–191, 10.1016/j.neuroscience.2020.05.050. [PubMed: 32512136]

[11]. KentC Berridge, IanQ Whishaw, Cortex, striatum and cerebellum: control of serial order in a grooming sequence, Exp. Brain Res 90 (1992), 10.1007/BF00227239.

[12]. Lemke SM, Ramanathan DS, Guo L, Won SJ, Ganguly K, Emergent modular neural control drives coordinated motor actions, Nat. Neurosci 22 (2019) 1122–1131, 10.1038/s41593-019-0407-2. [PubMed: 31133689]

[13]. Furuya S, Tominaga K, Miyazaki F, Altenmüller E, Losing dexterity: patterns of impaired coordination of finger movements in musician's dystonia, Sci. Rep 5 (2015) 13360, 10.1038/srep13360. [PubMed: 26289433]

[14]. Oktayoglu P, Acar A, Gunduz I, Caglayan M, Akbostanci MC, Assessment of hand functions in patients with idiopathic cervical dystonia, Hum. Mov. Sci 70 (2020), 102581, 10.1016/j.humov.2020.102581.

[15]. Balas M, Peretz C, Badarny S, Scott RB, Giladi N, Neuropsychological profile of DYT1 dystonia, Mov. Disord 21 (2006) 2073–2077, 10.1002/mds.21070. [PubMed: 17013905]

[16]. Kalueff AV, Stewart AM, Song C, Berridge KC, Graybiel AM, Fentress JC, Neurobiology of rodent self-grooming and its value for translational neuroscience, Nat. Rev. Neurosci 17 (2016) 45–59, 10.1038/nrn.2015.8. [PubMed: 26675822]

[17]. Kalueff AV, Aldridge JW, LaPorte JL, Murphy DL, Tuohimaa P, Analyzing grooming microstructure in neurobehavioral experiments, Nat. Protoc 2 (2007) 2538–2544, 10.1038/nprot.2007.367. [PubMed: 17947996]

[18]. Liang C-C, Tanabe LM, Jou S, Chi F, Dauer WT, TorsinA hypofunction causes abnormal twisting movements and sensorimotor circuit neurodegeneration, J. Clin. Invest 124 (2014) 3080–3092, 10.1172/JCI72830. [PubMed: 24937429]

[19]. Farr TD, Whishaw IQ, Quantitative and qualitative impairments in skilled reaching in the mouse (Mus musculus) after a focal motor cortex stroke, Stroke 33 (2002) 1869–1875, 10.1161/01.str.0000020714.48349.4e. [PubMed: 12105368]

[20]. Bova A, Gaidica M, Hurst A, Iwai Y, Hunter J, Leventhal DK, Precisely timed dopamine signals establish distinct kinematic representations of skilled movements, ELife 9 (2020), e61591, 10.7554/eLife.61591.

[21]. Berridge KC, Fentress JC, Disruption of natural grooming chains after striatopallidal lesions, Psychobiology 15 (1987) 336–342.

[22]. Alaverdashvili M, Moon S-K, Beckman CD, Virag A, Whishaw IQ, Acute but not chronic differences in skilled reaching for food following motor cortex devascularization vs. photothrombotic stroke in the rat, Neuroscience 157 (2008) 297–308, 10.1016/j.neuroscience.2008.09.015. [PubMed: 18848605]

[23]. Bova A, Ferris K, Leventhal DK, Evolution of gross forelimb and fine digit kinematics during skilled reaching acquisition in rats, Eneuro 8 (2021), 10.1523/ENEURO.0153-21.2021.

[24]. Ueno M, Nakamura Y, Li J, Gu Z, Niehaus J, Maezawa M, Crone SA, Goulding M, Baccei ML, Yoshida Y, Corticospinal circuits from the sensory and motor cortices differentially regulate skilled movements through distinct spinal interneurons, Cell Rep. 23 (2018) 1286–1300, 10.1016/j.celrep.2018.03.137. [PubMed: 29719245]

[25]. Klein A, Dunnett SB, Analysis of skilled forelimb movement in rats: the single pellet reaching test and staircase test, Unit8.28, Curr. Protoc. Neurosci (2012), 10.1002/0471142301.ns0828s58.

[26]. Berridge KC, Progressive degradation of serial grooming chains by descending decerebration, Behav. Brain Res 33 (1989) 241–253, 10.1016/S0166-4328(89)80119-6. [PubMed: 2757783]

[27]. Cromwell HC, Berridge KC, Drago J, Levine MS, Action sequencing is impaired in D1A-deficient mutant mice, Eur. J. Neurosci 10 (1998) 2426–2432, 10.1046/j.1460-9568.1998.00250.x. [PubMed: 9749770]

[28]. Cromwell HC, Berridge KC, Implementation of action sequences by a neostriatal site: a lesion mapping study of grooming syntax, J. Neurosci 16 (1996) 3444–3458, 10.1523/JNEUROSCI.16-10-03444.1996. [PubMed: 8627378]

[29]. Becker MI, Calame DJ, Wrobel J, Person AL, Online control of reach accuracy in mice, J. Neurophysiol 124 (2020) 1637–1655, 10.1152/jn.00324.2020. [PubMed: 32997569]

[30]. Parmiani P, Lucchetti C, Franchi G, Whisker and nose tactile sense guide rat behavior in a skilled reaching task, Front. Behav. Neurosci 12 (2018) 24, 10.3389/fnbeh.2018.00024. [PubMed: 29515377]

[31]. Whishaw IQ, Tomie JA, Olfaction directs skilled forelimb reaching in the rat, Behav. Brain Res 32 (1989) 11–21, 10.1016/s0166-4328(89)80067-1. [PubMed: 2930630]

[32]. Parmiani P, Lucchetti C, Franchi G, The effects of olfactory bulb removal on single-pellet skilled reaching task in rats, Eur. J. Neurosci 53 (2021) 827–840, 10.1111/ejn.15066. [PubMed: 33249662]

[33]. Ballermann M, Tompkins G, Whishaw IQ, Skilled forelimb reaching for pasta guided by tactile input in the rat as measured by accuracy, spatial adjustments, and force, Behav. Brain Res 109 (2000) 49–57, 10.1016/s0166-4328(99)00164-3. [PubMed: 10699657]

[34]. Fenrich KK, May Z, Hurd C, Boychuk CE, Kowalczewski J, Bennett DJ, Whishaw IQ, Fouad K, Improved single pellet grasping using automated ad libitum full-time training robot, Behav. Brain Res 281 (2015) 137–148, 10.1016/j.bbr.2014.11.048. [PubMed: 25523027]

[35]. Ellens DJ, Gaidica M, Toader A, Peng S, Shue S, John T, Bova A, Leventhal DK, An automated rat single pellet reaching system with high-speed video capture, J. Neurosci. Methods 271 (2016) 119–127, 10.1016/j.jneumeth.2016.07.009. [PubMed: 27450925]

[36]. DeSimone JC, Pappas SS, Febo M, Burciu RG, Shukla P, Colon-Perez LM, Dauer WT, Vaillancourt DE, Forebrain knock-out of torsinA reduces striatal free-water and impairs whole-brain functional connectivity in a symptomatic mouse model of DYT1 dystonia, Neurobiol. Dis 106 (2017) 124–132, 10.1016/j.nbd.2017.06.015. [PubMed: 28673740]

[37]. Aldridge JW, Berridge KC, Coding of serial order by neostriatal neurons: a “natural action” approach to movement sequence, J. Soc. Neurosci 18 (1998) 2777–2787.

[38]. Meyer-Luehmann M, Thompson JF, Berridge KC, Aldridge JW, Substantia nigra pars reticulata neurons code initiation of a serial pattern: implications for natural action sequences and sequential disorders, Eur. J. Neurosci 16 (2002) 1599–1608, 10.1046/j.1460-9568.2002.02210.x. [PubMed: 12405974]

[39]. Silberstein P, Kühn AA, Kupsch A, Trottenberg T, Krauss JK, Wöhrle JC, Mazzone P, Insola A, Di Lazzaro V, Oliviero A, Aziz T, Brown P, Patterning of globus pallidus local field potentials differs between Parkinson’s disease and dystonia, Brain J. Neurol 126 (2003) 2597–2608, 10.1093/brain/awg267.

[40]. Starr PA, Rau GM, Davis V, Marks WJ, Ostrem JL, Simmons D, Lindsey N, Turner RS, Spontaneous pallidal neuronal activity in human dystonia: comparison with Parkinson’s disease and normal macaque, J. Neurophysiol 93 (2005) 3165–3176, 10.1152/jn.00971.2004. [PubMed: 15703229]

[41]. Barow E, Neumann W-J, Brücke C, Huebl J, Horn A, Brown P, Krauss JK, Schneider G-H, Kühn AA, Deep brain stimulation suppresses pallidal low frequency activity in patients with phasic dystonic movements, Brain J. Neurol 137 (2014) 3012–3024, 10.1093/brain/awu258.

[42]. Pappas SS, Leventhal DK, Albin RL, Dauer WT, Mouse models of neurodevelopmental disease of the basal ganglia and associated circuits, Curr. Top. Dev. Biol 109 (2014) 97–169, 10.1016/B978-0-12-397920-9.00001-9. [PubMed: 24947237]

[43]. Sharma N, Baxter MG, Petravicz J, Bragg DC, Schienda A, Standaert DG, Breakefield XO, Impaired motor learning in mice expressing torsinA with the DYT1 dystonia mutation, J. Neurosci,. J. Soc. Neurosci 25 (2005) 5351–5355, 10.1523/JNEUROSCI.0855-05.2005.

[44]. Grundmann K, Reischmann B, Vanhoutte G, Hübener J, Teismann P, Hauser T-K, Bonin M, Wilbertz J, Horn S, Nguyen HP, Kuhn M, Chanarat S, Wolburg H, Van der Linden A, Riess O, Overexpression of human wildtype torsinA and human DeltaGAG torsinA in a transgenic mouse model causes phenotypic abnormalities, Neurobiol. Dis 27 (2007) 190–206, 10.1016/j.nbd.2007.04.015. [PubMed: 17601741]

[45]. Grundmann K, Glöckle N, Martella G, Sciamanna G, Hauser T-K, Yu L, Castaneda S, Pichler B, Fehrenbacher B, Schaller M, Nuscher B, Haass C, Hettich J, Yue Z, Nguyen HP, Pisani A, Riess O, Ott T, Generation of a novel rodent model for DYT1 dystonia, Neurobiol. Dis 47 (2012) 61–74, 10.1016/j.nbd.2012.03.024. [PubMed: 22472189]

[46]. Dang MT, Yokoi F, Pence MA, Li Y, Motor deficits and hyperactivity in Dyt1 knockdown mice, Neurosci. Res 56 (2006) 470–474, 10.1016/j.neures.2006.09.005. [PubMed: 17046090]

[47]. Yokoi F, Dang MT, Mitsui S, Li J, Li Y, Motor deficits and hyperactivity in cerebral cortex-specific Dyt1 conditional knockout mice, J. Biochem. (Tokyo) 143 (2008) 39–47, 10.1093/jb/mvm191. [PubMed: 17956903]

[48]. Yokoi F, Dang MT, Li J, Standaert DG, Li Y, Motor deficits and decreased striatal dopamine receptor 2 binding activity in the striatum-specific Dyt1 conditional knockout mice, PloS One 6 (2011), e24539, 10.1371/journal.pone.0024539.

[49]. Sciamanna G, Hollis R, Ball C, Martella G, Tassone A, Marshall A, Parsons D, Li X, Yokoi F, Zhang L, Li Y, Pisani A, Standaert DG, Cholinergic dysregulation produced by selective inactivation of the dystonia-associated protein torsinA, Neurobiol. Dis 47 (2012) 416–427, 10.1016/j.nbd.2012.04.015. [PubMed: 22579992]

[50]. Carbon M, Argyelan M, Ghilardi MF, Mattis P, Dhawan V, Bressman S, Eidelberg D, Impaired sequence learning in dystonia mutation carriers: a genotypic effect, Brain 134 (2011) 1416–1427, 10.1093/brain/awr060. [PubMed: 21515903]

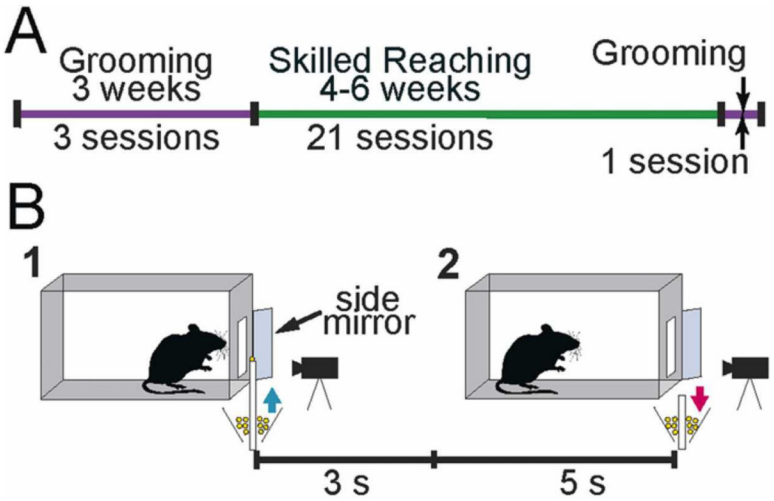

Fig. 1.

Experimental overview. A): Timeline for a complete set of experiments on a single mouse. B) Timeline for a single skilled reaching trial. (1) – the pedestal rises, bringing a sugar pellet into position to allow reaching, where it stays for 3 s before (2) – the pedestal descends to retrieve a new pellet for the next trial.

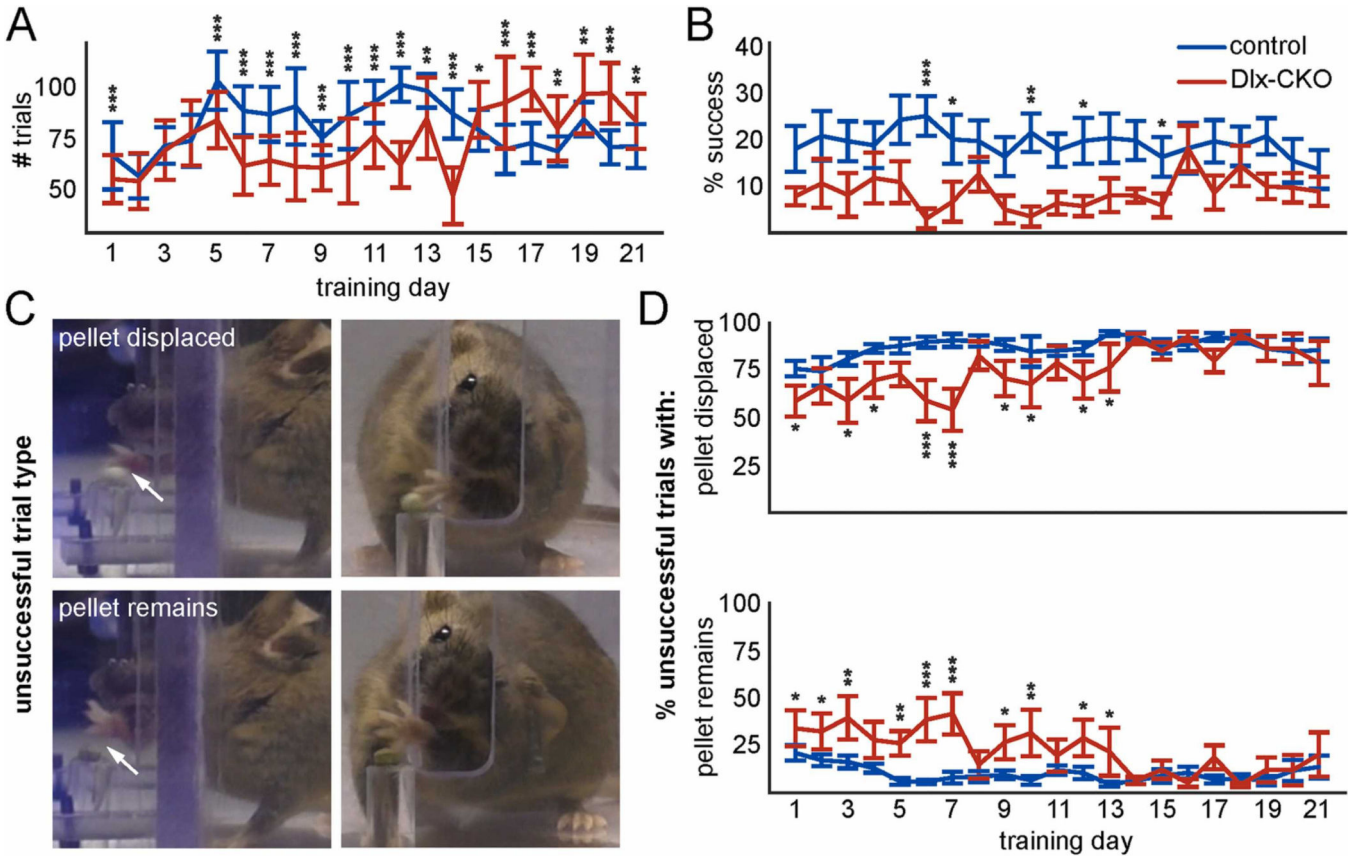

Fig. 2.

Dlx-CKO mice are impaired in skilled reaching (n = 23; control=14, Dlx-CKO=9). A) Number of trials in which mice performed at least one reach. Generalized linear model: effect of genotype: z = − 7.54, $p = 4.8 \times 10^{-14}$; effect of session: z = 0.197, p = 0.84; interaction between genotype and session: z = 11.7, $p < 2.0 \times 10^{-16}$ B) Average "any attempt" success rate. Linear mixed-effects model: effect of genotype: F(1,21)= − 2.48, p = 0.022; effect of session: F(2,20)= − 0.507, p = 0.62; interaction between genotype and session: F(3,19)= 0.657, p = 0.52. Asterisks indicate a significant difference between experimental groups in specific sessions. C) Still image of a control mouse at maximum paw extension during an unsuccessful trial in which the paw contacted the pellet, displacing it (Top) and in which the paw missed the pellet, allowing it to remain on the pedestal (Bottom). Arrows indicate the closest distance between paw and pellet. D) Fraction of unsuccessful trials during which mice displaced (Top; "pellet displaced") or did not displace (Bottom; "pellet remained") the pellet. Asterisks indicate a significant difference between groups in specific sessions. Linear mixed-effects model for "pellet displaced" trials: effect of genotype: F(7,15)= − 3.80, $p = 1.7 \times 10^{-3}$; effect of session: F(4,18)= 1.33, p = 0.20; interaction between genotype and session: F(4,18)= 2.10, p = 0.050. Linear mixed-effects model for "pellet remains" trials: effect of genotype: F(5,17)= 4.49, $p = 3.3 \times 10^{-4}$; effect of session: F(3,19)= − 1.00, p = 0.33; interaction between genotype and session: F(4,18)= − 2.14, p = 0.046. For individual sessions in panels A, B, and D, * indicates $p < 0.05$; * *

indicates $p < 0.01$; * ** indicates $p < 0.001$. Error bars represent mean +/− SEM. The full statistical tables are provided in Supplemental Data 1.

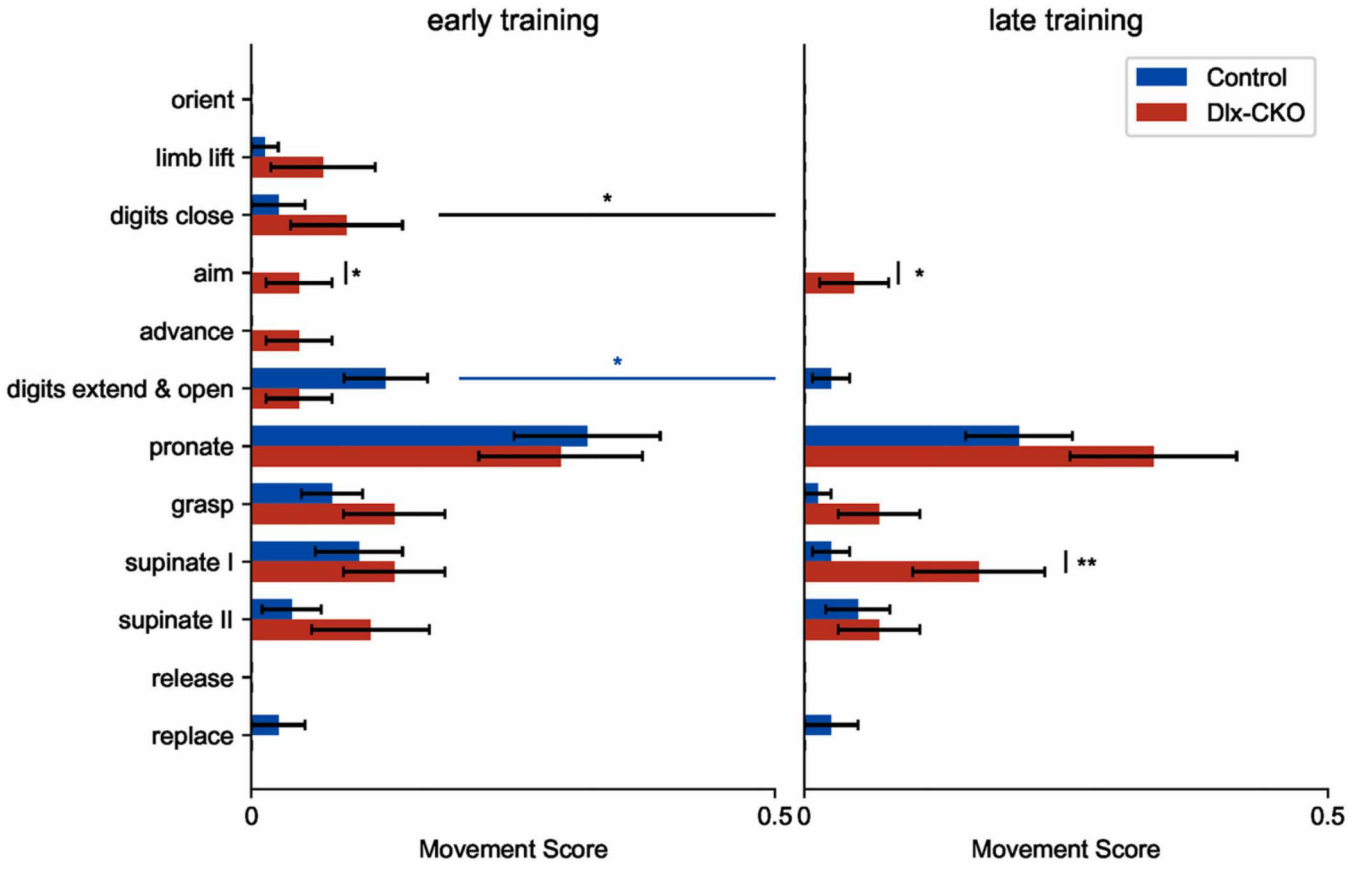

Fig. 3.

Movement element scores are similar between Dlx-CKO and control mice (n = 23; control=14, Dlx-CKO=9). Mean movement element scores for the first 3 correct reaches (early training) and last 3 correct reaches (late training). Two-way mixed-effects ANOVA: Main effect of genotype on “aim”: $F(3,19) = 5.89$, $p = 0.025$; Main effect of genotype on “supinate I”: $F(3,19) = 5.05$, $p = 0.037$. Main effect of training on “digits close”: $F(3,19) = 5.24$, $p = 0.034$; Main effect of training on “digits extend and open”: $F(3,19) = 8.23$, $p = 0.010$. Lines linking early to late training indicate significant changes from early to late training. Bars over a specific movement element indicate a difference between genotypes. Black lines indicate main effects. Colored lines represent effects specific to one genotype. * indicates $p < 0.05$. Error bars represent mean + /− SEM. The full statistical tables are reported in Supplemental Data 2.

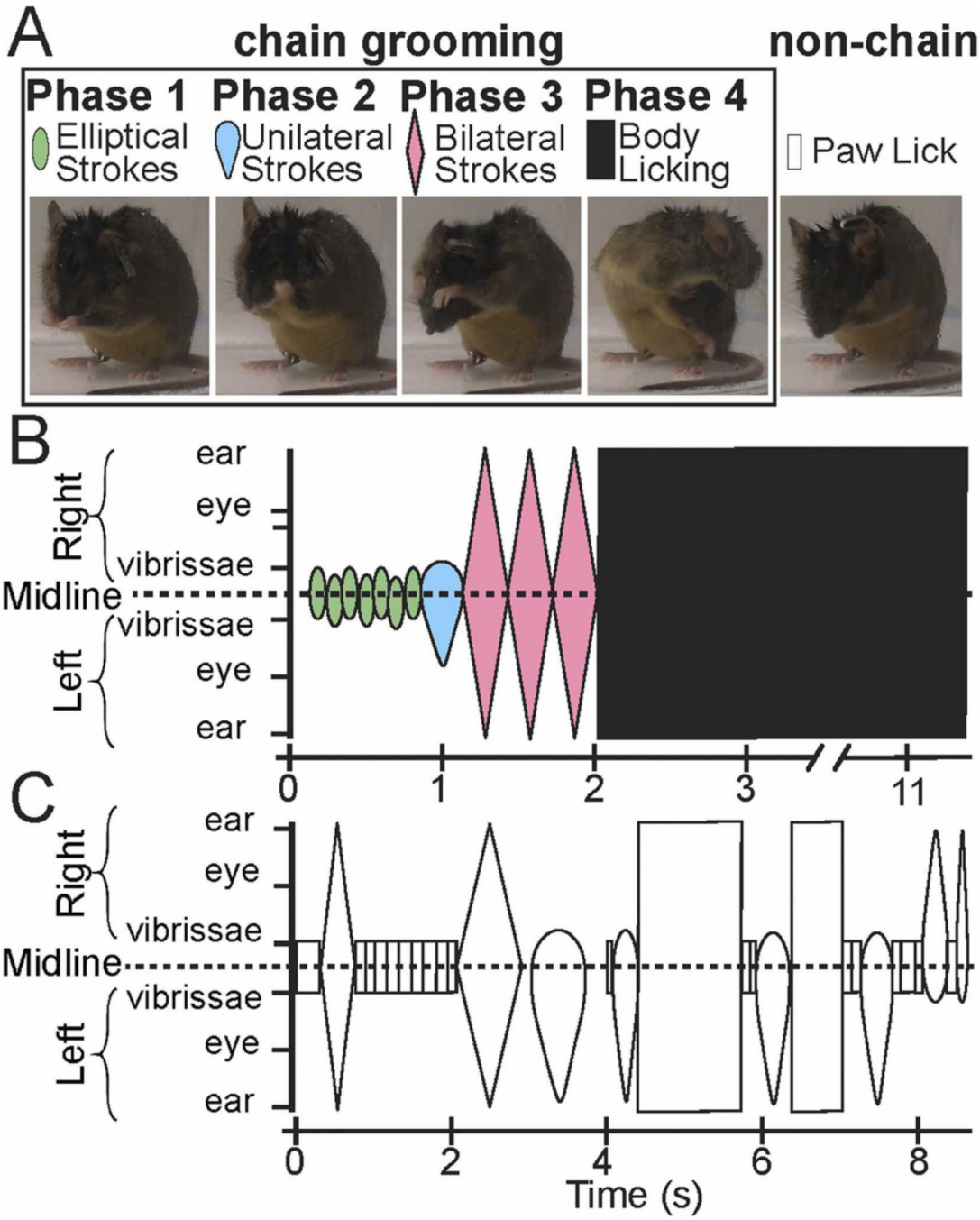

Fig. 4.

Grooming structure in control mice. A) Mouse grooming consists of syntactic chains, made up of stereotyped strokes, which are usually embedded in longer and less stereotyped non-chain grooming bouts. Stroke types are similar in chain and non-chain grooming with the exception of paw licks, which do not occur in chain grooming. Shapes correspond to forelimb stroke types, and colors correspond to syntactic chain phases. *Elliptical strokes* consist of small bilateral strokes near the nose. *Unilateral strokes* consist of larger elliptical motions from the vibrissae to the snout that occur asynchronously. *Bilateral strokes* are

similar to unilateral strokes, but occur synchronously in both arms. *Body licking* consists of body twisting so the mouse can clean its haunches. *Paw licks* consist of paw licking without small elliptical strokes. B) Choreography of a complete syntactic chain. Individual symbols indicate the stroke type, and their size represents the amplitude of the movement with respect to facial landmarks. C) Choreography of a non-chain grooming bout. Transitions between stroke types occur at a slower pace and in a less predictable order.

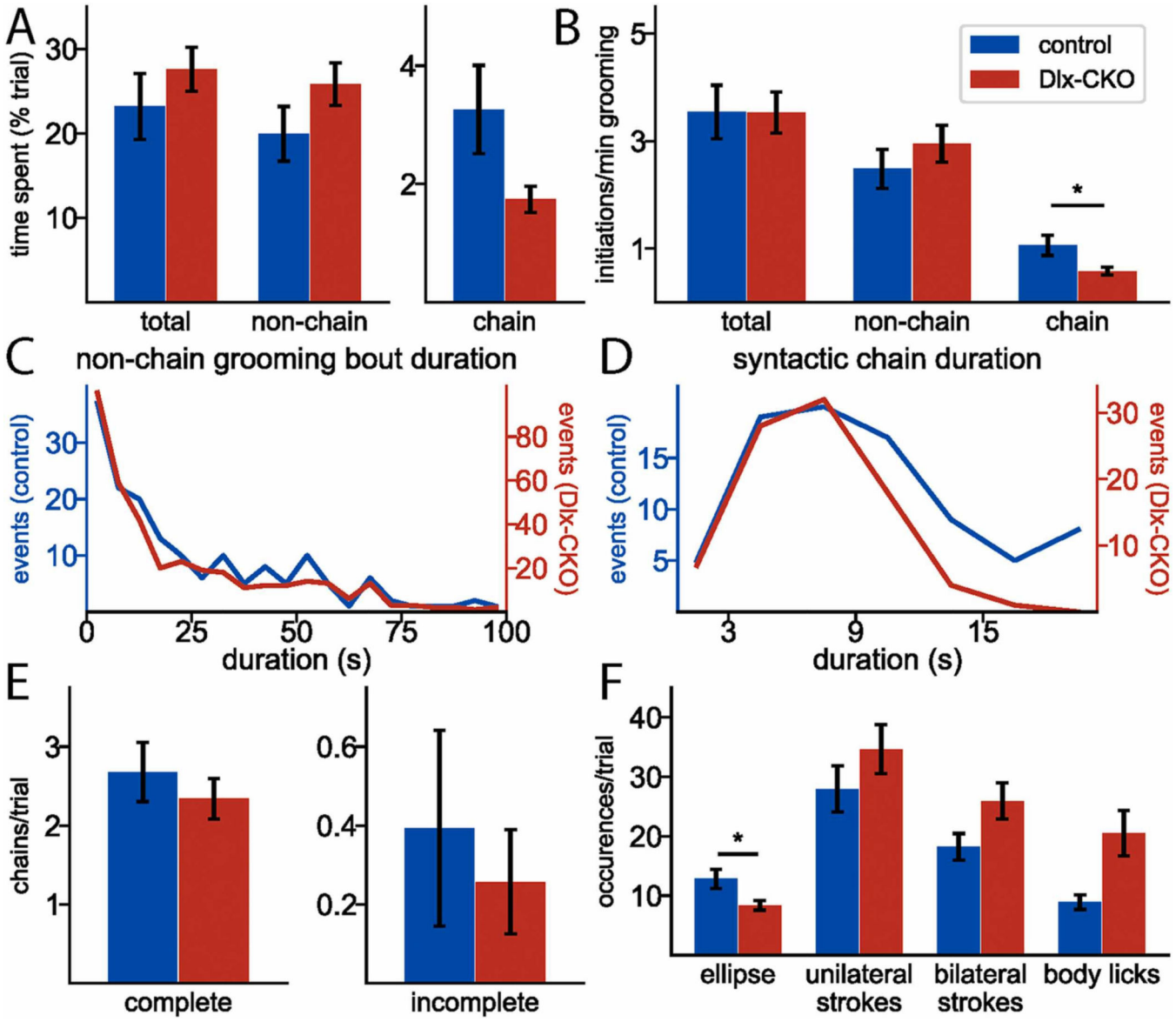

Fig. 5.

Dlx-CKO mice perform similar amounts of grooming, but in more variable patterns, than controls (control=5, Dlx-CKO=8). A) Time spent grooming in total, in non-chain bouts, and in chain bouts. Linear Regression, effect of genotype: total time spent grooming: $t(12) = 0.053$, $p = 0.96$; time spent non-chain grooming $t(12) = 1.40$, $p = 0.19$; time spent chain grooming: $t(12) = \_ 1.93$, $p = 0.079$. B) Number of bout initiations per minute of grooming in total, for non-chain grooming, and for chain grooming. Kruskal-Wallis test, effect of genotype: non-chain bout initiation: chi- squared= 2.49, df= 1, $p = 0.11$; syntactic chain initiation: chi-squared= 4.83, df= 1, $p = 0.028$. C & D) Distribution of non-chain (C) and syntactic chain (D) grooming bout durations. The left and right axes represent counts for control and Dlx-CKO mice, respectively. Axes were scaled to maximum counts to facilitate comparison. E) Number of complete and incomplete syntactic chains per trial. Poisson Regression, effect of genotype on: number complete syntactic chains: $z(12) = 0.49$, $p = 0.63$;

number incomplete syntactic chains: z(12) = − 1.05, p = 0.29. F) Frequency of performance of each grooming phase. Kruskall-Wallis test, effect of genotype: ellipses: chi-squared= 4.16, df= 1, p = 0.041; unilateral strokes: chi- squared= 0.99, df= 1, p = 0.32; bilateral strokes: chi-squared= 2.26, df= 1, p = 0.13; body licks: chi-squared= 1.86, df= 1, p = 0.17. * indicates $p < 0.05$ for a main effect of genotype for each trial outcome. # indicates $p < 0.05$ for a main effect of session number for each trial outcome. The full statistical tables are reported in Supplemental Data 3.